ACI STRUCTURAL JOURNAL TECHNICAL PAPER

Title no. 98-S38

Stress-Strain Behavior of High-Strength Concrete Confined by Ultra-High- and Normal-Strength Transverse Reinforcements

by Li Bing, R. Park, and H. Tanaka

When high-strength concrete is used for reinforced concrete members subjected to seismic loading, it is more difficult to achieve ductile behavior of such members than when normal-strength concrete is used. In this paper, an experimental study of a number of quasi-static axial loading tests on high-strength concrete specimens confined by various amounts of transverse reinforcement is described. The main parameters were concrete strengths ranging from 35.2 to 82.5 MPa and yield strength of Grade 430 and 1300 transverse reinforcement. A stress-strain relationship for confined high-strength concrete is proposed that is found to give reasonably good prediction of the experimental behavior of circular and square specimens with high-strength concrete confined by either normal- or ultra-high-yield-strength with various configurations. An empirical formula for the ultimate longitudinal strain of confined high-strength concrete corresponding to the first hoop or spiral fracture is also proposed.

Keywords: column; confinement reinforcement; high-strength concrete; strains; stresses; tests.

INTRODUCTION

Reinforced concrete buildings are generally designed to behave in a ductile manner under the action of a severe earthquake. To achieve such ductile behavior, structural members of the buildings should be carefully detailed. In the case of buildings with moment-resisting frames, detailing of transverse reinforcement in the potential plastic hinge regions of the columns is a major consideration. For many years researchers have been investigating a method for detailing the transverse reinforcement to increase strength and ductility of reinforced concrete columns. It has been demonstrated that adequate confinement of the core concrete and tying of longitudinal reinforcement using transverse reinforcement can improve column ductility most effectively. Past and recent earthquakes have proved the validity of this philosophy.

The gradual development of concrete technology has promoted the use of high-strength concrete in the construction industry. Concrete technology has developed to an extent where concrete compressive strengths up to 100 MPa and higher can be reached without difficulties. There are, however, only a limited number of studies relating to the confining effects on high-strength concrete, even though the use of high-strength concrete has been increasing in recent years. Meanwhile, the strength of reinforcing steel has also been improved markedly. Normally the yield strength of reinforcement is approximately 300 to 500 MPa. Ultra-high-strength reinforcement with yield strength over 1000 MPa, however, has been recently used for transverse reinforcement of concrete columns in Japan. Some research work has shown that the use of ultra-high-strength steel for transverse reinforcement can effectively increase the ductility of reinforced concrete columns. Ultra-high-strength transverse reinforcement is especially used for columns with high-strength concrete.

RESEARCH SIGNIFICANCE

The most fundamental issue in predicting the behavior of reinforced concrete members is the stress-strain behavior of the constituent materials. Concrete is used to resist compression and its behavior in compression is important to the designer. If the behavior of concrete subjected to uniaxial compression is known, the flexural behavior of reinforced concrete can be estimated. The confinement steel requirements for normal-strength concrete are reasonably well established in current building codes. In recent years, the possible use of high-strength concrete for buildings constructed using reinforced concrete has been considered. Research findings for high-strength concrete, however, are relatively scarce in the literature.

SUMMARY OF MODELS

A number of stress-strain models have been proposed in the past 15 years. A detailed review of existing models was presented elsewhere.[1] The following section provides an overview of these analytical models that cover high-strength concrete.

Martinez, Nilson, and Slate (1982)

Martinez, Nilson, and Slate[2] conducted experiments on several small diameter cylindrical specimens of high-strength concrete confined by spiral reinforcement without concrete cover and longitudinal reinforcement. The concrete strength of the specimens ranged from 21 to 69 MPa and the confining pressure ranged from 1.7 to 2.1 MPa. The yield strength of the lateral reinforcement was approximately 414 MPa. They proposed a theoretical model for the complete stress-strain curve of spirally confined high-strength concrete columns based on their own test results.

Fafitis and Shah (1985)

Fafitis and Shah[3] tested a large number of small concrete cylinders with practically no cover to the spiral steel and had no longitudinal reinforcement. The spiral wire was 3.2 mm

ACI Structural Journal, V. 98, No. 3, May-June 2001.
MS No. 00-135 received June 6, 2000, and reviewed under Institute publication policies. Pertinent discussion will be published in the March-April 2002 *ACI Structural Journal* if received by November 1, 2001.

Li Bing *is an assistant professor in the School of Civil and Structural Engineering at the Nanyang Technological University, Singapore. He received his BE from Tong Ji University, China, and his PhD from the University of Canterbury, New Zealand. His research interests include reinforced concrete, precast concrete structures, and designing for earthquake resistance and blast loading.*

R. Park, *FACI, is an Emeritus Professor of civil engineering at the University of Canterbury, New Zealand. He is a corecipient of ACI's 1984 and 1989 Raymond C. Reese Research Award. His research interests include reinforced and prestressed concrete structures, and designing for earthquake resistance.*

H. Tanaka *is a professor in the Disaster Prevention Research Institute, Kyoto University, Japan. He received his BE and ME from Kyoto University, Japan, and his PhD in civil engineering from the University of Canterbury. His research interests include reinforced concrete and high-strength concrete structures, particularly designing for earthquake resistance.*

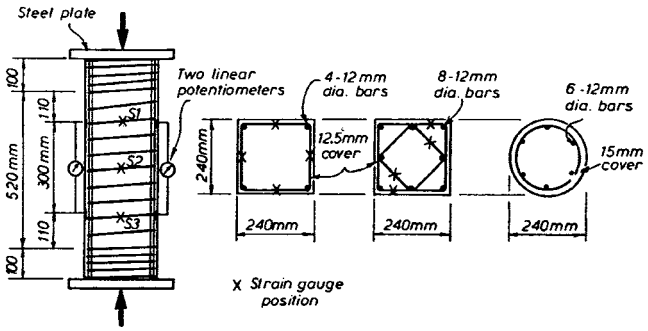

Fig. 1—Short column with axial compressive loading: principal dimensions; test setup; instrumentation; and position of strain gages.

in diameter and had a yield strength of 413 MPa. Variables investigated in the experiment included the concrete compressive strength, the spiral spacing, and the strain rate effect (slow and fast). Based on their test results and the results of Martinez, Nilson, and Slate,[2] Fafitis and Shah proposed a theoretical model for the complete stress-strain curve of circular and square confined high-strength concrete.

Yong, Nour, and Nawy (1989)

Yong, Nour, and Nawy[4] tested 24 square prisms (152 x 152 x 457 mm) that were made of high-strength concrete with compressive strengths ranging from 83.6 to 93.5 MPa, confined with square hoops with a yield strength of 496 MPa. Based on their test results, Yong, Nour, and Nawy proposed a three-part stress-strain curve for rectilinear confined concrete.

Bjerkeli, Tomaszewicz, and Jansen (1990)

Bjerkeli, Tomaszewicz, and Jansen[5] tested a large number of plain and confined high-strength concrete columns (150 mm diameter x 500 mm high cylinders, 150 x 150 x 500 mm prisms, and 300 x 500 x 2000 mm prisms) confined with various volumetric ratios of spiral reinforcement. The concrete compressive strengths ranged from 65 to 115 MPa. The test specimens contained longitudinal steel but no concrete cover. They proposed a three-part stress-strain curve for confined high-strength concrete based on their test results.

Muguruma and Watanabe (1992)

Muguruma and Watanabe[6] tested small square specimens confined laterally by square helix hoops of different yield strengths and with various volumetric ratios. The specimens contained no longitudinal reinforcement and had no cover. The concrete strength of the specimen was varied from 31.5 to 87.5 MPa. The yield strength of hoops ranged from 191 to 1397 MPa. Based on their experimental work, they proposed a three-part stress-strain curve.

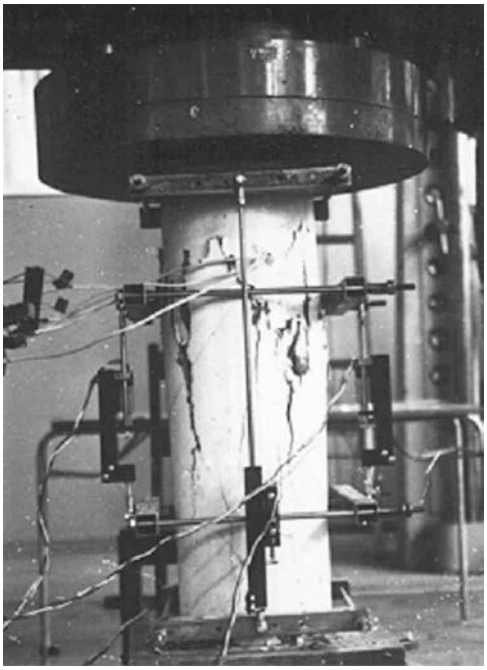

Fig. 2—Test units set up in 10 MN capacity hydraulic universal testing machine.

Cusson and Paultre (1995)

Cusson and Paultre[7] have developed a stress-strain model and calibrated it against their experimental results from high-strength concrete tied columns. All the tested specimens were 235 x 235 x 1400 mm. The concrete strength considered in the experimental program ranged from 60 to 120 MPa and the yield strength of confinement steel ranged between 400 to 800 MPa.

Razvi and Saatcioglu (1996)

Razvi and Saatcioglu[8] developed a stress-strain model for confined high-strength concrete based on their tests conducted on a large number of near-full size circular and square column specimens. The concrete strength considered in the experimental program ranged from 60 to 124 MPa and the yield strength of confinement steel ranged between 400 to 1000 MPa.

Most of the models show very similar trends that indicates any one of them could be used to generally predict the behavior of high-strength concrete, if properly calibrated.

EXPERIMENTAL PROGRAM

A total of 40 reinforced concrete columns 720 mm in length were tested. They were either 240 mm square or 240 mm diameter circular sections. The arrangement of longitudinal bars, transverse hoops, square helices, and spiral reinforcement used are given in Fig. 1. The reinforcement details are listed in Table 1 and 2. Four different concrete compressive strengths were used, ranging from 35.2 to 82.5 MPa. Two grades of transverse reinforcement were used in the test units, namely Grade 430 steel (f_{yh} = 445 MPa) and ultra-high Grade 1300 steel (f_{yh} = 1318 MPa). The hoop bars were anchored by a 135-degree bend around longitudinal bars. They were extended beyond the bend of at least eight hoop bar diameters in the concrete core. The

Table 1—Specimen properties for square test units

Unit no.	f'_{co}, MPa	Longitudinal reinforcement			Transverse reinforcement			
		No. of bars	Diameter, mm	f_y, MPa	Diameter, mm	Spacing, mm	f_{yh}, MPa	ρ_s, %
1A	60.0	4	12	443	6.0	20	445	2.63
1B	72.3	4	12	443	6.0	20	445	2.63
2A	60.0	8	12	443	6.0	20	445	4.48
2B	72.3	8	12	443	6.0	20	445	4.48
4A	60.0	4	12	443	6.0	35	445	1.50
4B	72.3	4	12	443	6.0	35	445	1.50
5A	60.0	8	12	443	6.0	35	445	2.56
5B	72.3	8	12	443	6.0	35	445	2.56
7A	60.0	4	12	443	6.0	50	445	1.05
7B	72.3	4	12	443	6.0	50	445	1.05
8A	60.0	8	12	443	6.0	50	445	1.79
8B	72.3	8	12	443	6.0	50	445	1.79
10A	60.0	4	12	443	6.0	65	445	0.80
10B	72.3	4	12	443	6.0	65	445	0.80
11A	60.0	8	12	443	6.0	65	445	1.38
11B	72.3	8	12	443	6.0	65	445	1.38
1HA	35.2	8	12	443	6.4	35	1318	2.86
1HB	52.0	8	12	443	6.4	20	1318	5.00
1HC1	82.5	8	12	443	6.4	20	1318	5.00
3HA	35.5	8	12	443	6.4	53	1318	1.89
3HB1	52.0	8	12	443	6.4	35	1318	2.86
3HB3	52.0	8	12	443	6.4	35	1318	2.86
3HC1	82.5	8	12	443	6.4	35	1318	2.86
3HC3	82.5	8	12	443	6.4	35	1318	2.86
5HA	35.5	8	12	443	6.4	70	1318	1.43
5HB	52.0	8	12	443	6.4	50	1318	2.00
5HC	82.5	8	12	443	6.4	50	1318	2.00

Table 2—Specimen properties for circular test units

Unit no.	f'_{co}, MPa	Longitudinal reinforcement			Transverse reinforcement			
		No. of bars	Diameter, mm	f_y, MPa	Diameter, mm	Spacing, mm	f_{yh}, MPa	ρ_s, %
3A	63.0	6	12	443	6.0	20.0	445	1.53
3B	72.3	6	12	443	6.0	20.0	445	1.53
6A	63.0	6	12	443	6.0	35.5	445	0.82
6B	72.3	6	12	443	6.0	35.5	445	0.82
9A	63.0	6	12	443	6.0	50.0	445	1.68
9B	72.3	6	12	443	6.0	50.0	445	1.68
12A	63.0	6	12	443	6.0	65.0	445	2.94
12B	72.3	6	12	443	6.0	65.0	445	2.94
2HA	35.2	6	12	443	6.4	35.0	1318	1.68
2HB	52.0	6	12	443	6.4	20.0	1318	2.94
2HC1	82.5	6	12	443	6.4	20.0	1318	2.94
4HA	35.2	6	12	443	6.4	53.0	1318	1.10
4HB1	52.0	6	12	443	6.4	35.0	1318	1.67
4HC	82.5	6	12	443	6.4	35.0	1318	1.67
6HA	35.2	6	12	443	6.4	70.0	1318	0.84
6HB	52.0	6	12	443	6.4	50.0	1318	1.17
6HC	82.5	6	12	443	6.4	50.0	1318	1.17

spacing of transverse hoops and helices was reduced to 25 mm within the region of 100 mm from each end of the test units to provide extra confinement and to ensure that failure occurs in the central region.

Concentric vertical load was provided by a 10 MN capacity hydraulic universal testing machine. The machine can be controlled by load, displacement, or strain. The steel reaction columns of the machine are stiff enough to permit the machine to measure the descending-branch of the load-deformation curve of the test specimens. Two different methods of recording axial deformations were used during testing of the specimens. The first method was to measure the overall shortening of the spec-

Table 3—Mixture proportions for different compressive strengths of concrete

Contents	Weights, m^3			
	f_c' = 35 MPa	f_c' = 52 MPa	f_c' = 75 MPa	f_c' = 82.5 MPa
13 mm aggregate	1210 kg	1150 kg	1150 kg	1188 kg
Kaiapoi sand	370 kg	600 kg	600 kg	495 kg
Yaldhurst sand	150 kg	150 kg	160 kg	124 kg
Ordinary portland cement	308 kg	400 kg	410 kg	400 kg
High-range water-reducing admixture	1.5 L	2.0 L	2.5 kg	2.5 L
Water	195 L	160 L	160 L	138 L
Silica fume solid	—	—	—	40 kg
Water-cement ratio	0.630	0.400	0.390	0.345

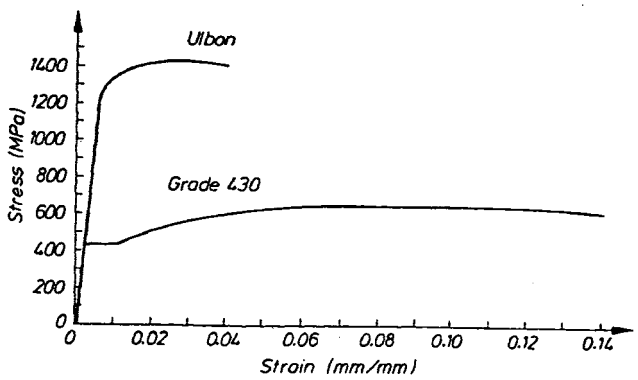

Fig. 3—Typical stress-strain curves for normal-yield-strength steel and high-yield-strength steel.

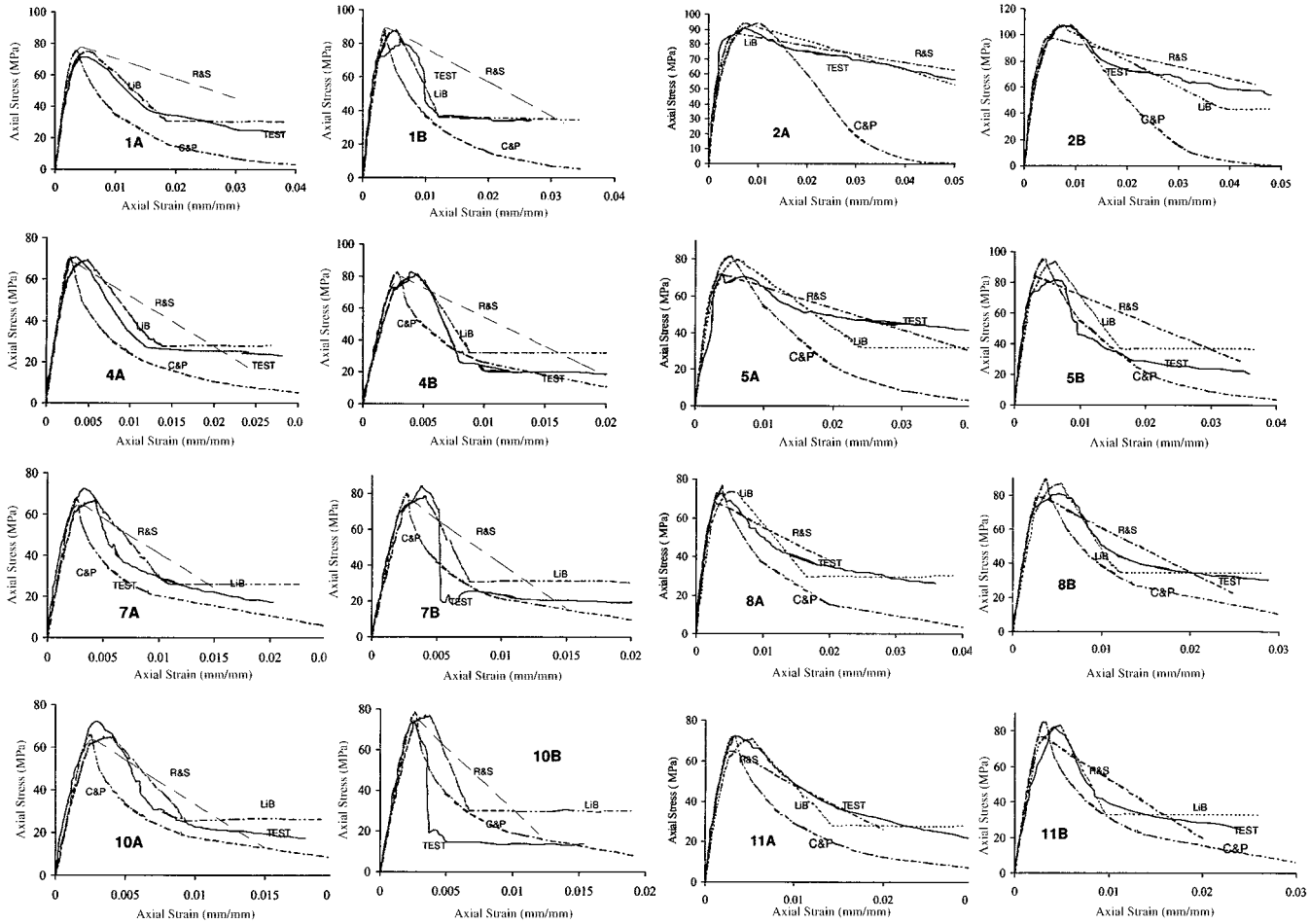

Fig. 4—Comparison of experimental and analytical curves for square cross sections confined by normal-yield-strength steel.

imen between the platen and the crosshead. The second method used four linear potentiometers of two different gage lengths to measure the axial strain of the specimen. Two 50 mm travel linear potentiometers were used to measure strains over the anticipated failure regions (central part of the specimen), that is, gage length of approximately 300 mm. Two other linear potentiometers were used to measure strains over the specimen's length from 40 mm from the top to 40 mm from the bottom of the specimen (a 640 mm gage [Fig. 2]). If a diagonal shear plane formed, this larger gage length could be used instead of the gage length over the central part of the specimen.

MATERIALS

A local ready-mix plant supplied the high-strength concrete used for the test units. The mixture proportions are shown in Table 3. The measured slumps of the concrete were all approximately 120 mm. A typical stress-strain curve of the reinforcement used is shown in Fig. 3.

GENERAL DESCRIPTION OF TEST BEHAVIOR

The measured stress-strain curves of confined concrete are shown in Fig. 4 to 7. The previous theoretical curves determined by Fafitis and Shah,[3] Yong, Nour, and Nawy,[4] Bjerkeli, Tomaszewicz, and Jansen,[5] Muguruma and Watanabe,[6] Cusson

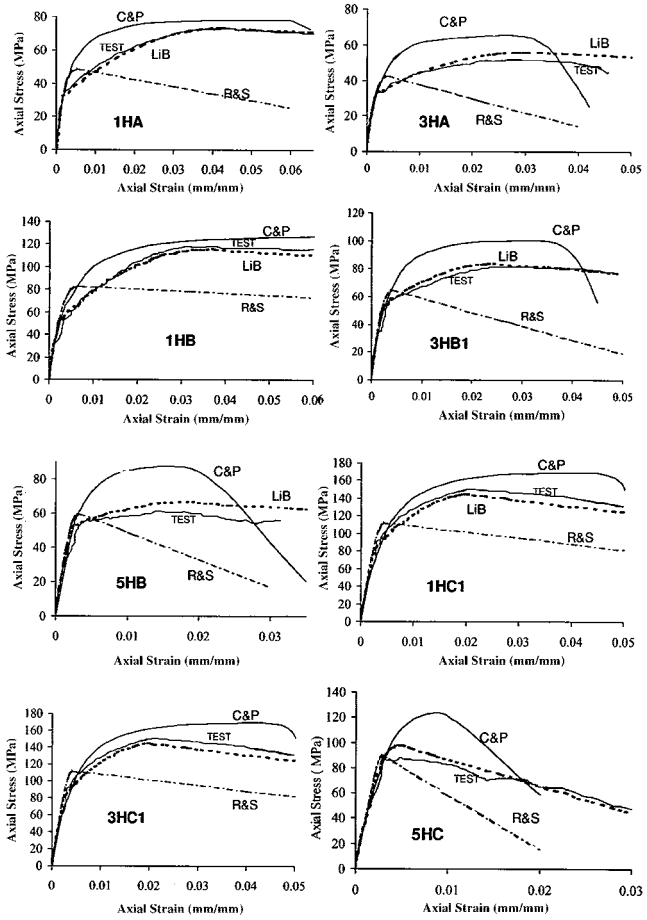

Fig. 5—Comparison of experimental and analytical curves for square cross section confined by ultra-high-yield-strength (f_{yh} = 1318 MPa) steel.

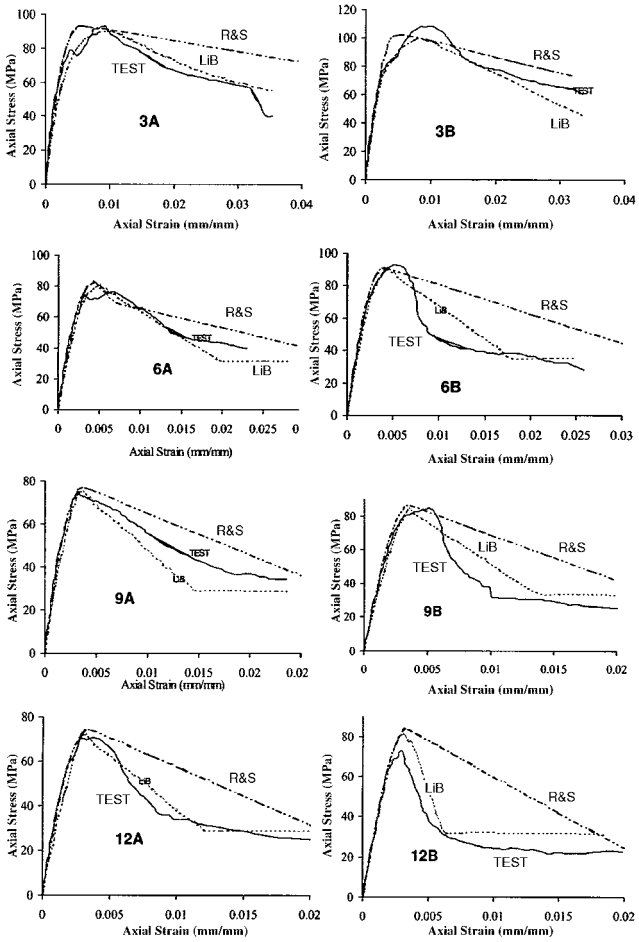

Fig. 6—Comparison of experimental and analytical curves for circular cross section confined by normal-yield-strength steel.

and Paultre,[7] and Razvi and Saatcioglu[8] were compared with some experimentally derived stress-strain curves (Fig. 8). Stress-strain curves predicted by models of Fafitis and Shah, Yong et al., Bjerkeli et al., Muguruma et al., Cusson and Paultre, and Razvi and Saatcioglu are denoted by F&S, Yong, BJ, MU, C&P, and R&S, respectively. A comparative study showed that most of the empirical models are effective only in interpreting their own test results or selected data. In comparing these models with experimental results obtained from this study, it was found that the models could not predict accurately the descending branch of the stress-strain curve of confined high-strength concrete. In seismic design, knowledge of the descending branch is very important to ensure proper behavior of columns, which undergo large deformations during an earthquake. The level of strength and ductility depends very much on the slope of the descending branch. Effects of concrete compressive strength, transverse reinforcement strength, and the amount of confining reinforcement on confined high-strength concrete are investigated.

The most significant parameters affecting the shape of the stress-strain curve of confined high-strength concrete for all section shapes are the volumetric ratio and the yield strength of the confining reinforcement. As the yield strength of the confining reinforcement is increased, both the strength and ultimate longitudinal strain of the confined concrete increased, while the slope of the falling branch decreased. The ultimate concrete longitudinal strain was defined as the strain at first hoop or spiral fracture.

The effect of a change in compressive strength of plain concrete f'_{co} on the degree of ductility of columns is significant, particularly for f'_{co} exceeding 60 MPa. Regardless of the concrete compressive strength, an increase in the confinement ratio increases the peak stress attained, increases the ultimate strain at first hoop or spiral fracture, and decreases the slope of the descending branch. An increasing spacing of transverse reinforcement tends to reduce the efficiency of the confinement. The failure of the normal- and high-strength concrete specimens confined by transverse reinforcement with high yield strength steel was sudden, violent, and explosive. This is because the transverse reinforcement fractured when the longitudinal bars buckled at very high strain, and the core concrete was crushed explosively due to a lack of confinement (Fig. 9). Consequently the specimen lost all of its load capacity. In contrast, the failure observed for specimens confined by normal yield strength steel was usually gradual and quite gentle after the first transverse bar fractured (Fig. 10). In axial loading tests of normal- and high-strength concrete cylinders and prisms confined by spirals or square helices with two different yield strengths of transverse reinforcement, namely, Grade 430 and 1300 steel, the strength and ductility of the confined concrete were enhanced when high yield steel was used.

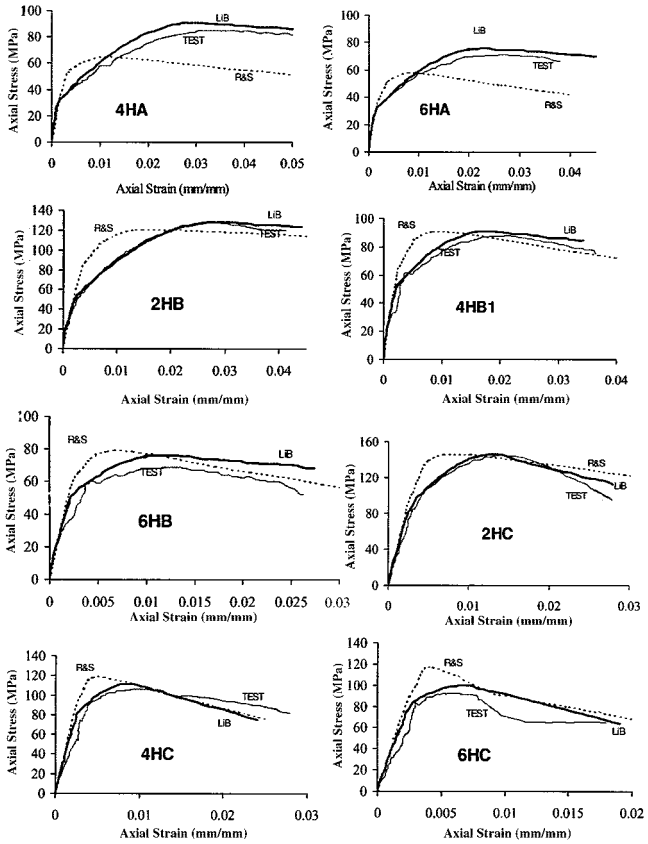

Fig. 7—Comparison of experimental and analytical curves for circular cross section confined by ultra-high-yield-strength (f_{yh} = 1318 MPa) steel.

DISCUSSION OF TEST RESULTS

Effect of concrete compressive strength

Concrete compressive strength is a significant factor on the behavior of confined concrete, as can been seen in the test results. For example, comparing 8A and 8B in Fig. 4, which have the same volumetric ratio of confining reinforcement but with different concrete compressive strengths, the test results indicated that the confinement effectiveness in term of axial strains was less with a higher concrete compressive strength. This is because the lateral dilation of high-strength concrete was smaller than that of normal-strength concrete.

Referring to the studies of Mander, Priestley, and Park[9] for normal-strength concrete confined by normal yield strength transverse steel, the equation for design purpose can be approximated as

$$f'_{cc} = f'_{co} + 5.5f'_l \quad (1)$$

In this study, for high-strength concrete confined by rectilinear or circular normal yield strength confining reinforcement, the equation for design purpose can be approximated as

$$f'_{cc} = f'_{co} + 4.0f'_l \quad (2)$$

For concrete with typical level of rectilinear or circular ultra high yield strength confining reinforcement, the following equations for design purposes can be approximated as:

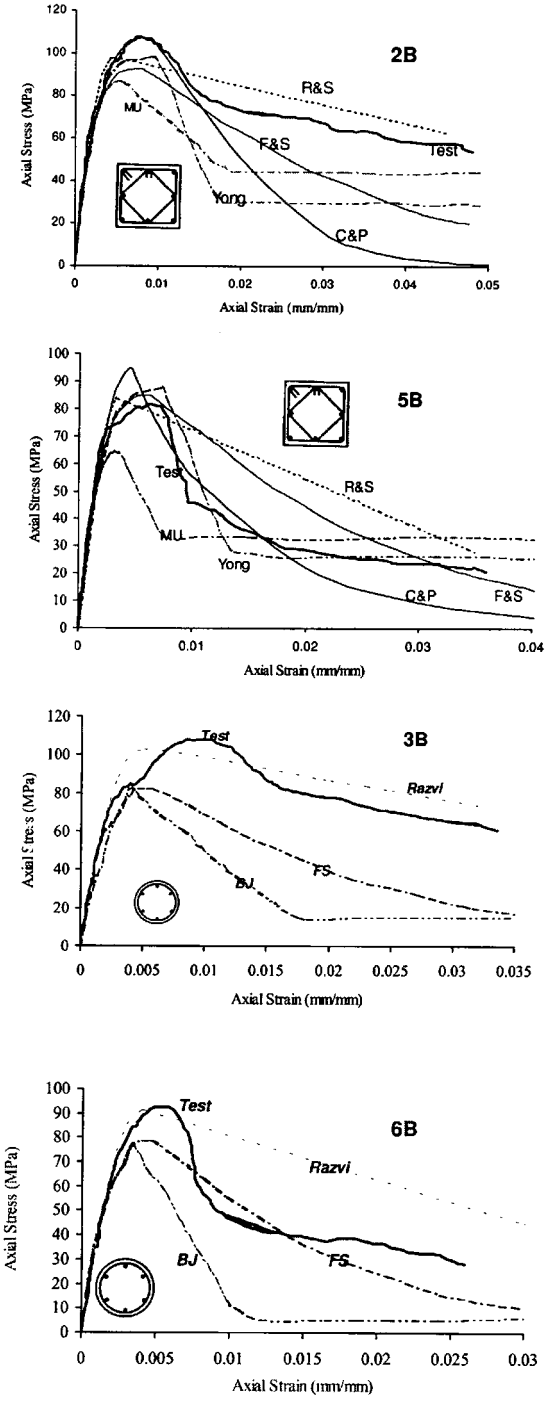

Fig. 8—Theoretical normalized stress-strain curves for confined concrete using different models compared with specimens.

Circular confinement— For normal-strength concrete

$$f'_{cc} = f'_{co} + 4.6f'_l \quad (3)$$

For high-strength concrete

$$f'_{cc} = f'_{co} + 2.7f'_l \quad (4)$$

Rectilinear confinement— For normal-strength concrete

$$f'_{cc} = f'_{co} + 2.1f'_l \quad (5)$$

Fig. 9—Specimens with ultra-high-strength (f_{yh} = 1318 MPa) confining reinforcement after testing.

For high-strength concrete

$$f'_{cc} = f'_{co} + 1.9f'_l \quad (6)$$

Effect of yield strength of transverse reinforcement

In this study, almost all gages on the Grade 430 steel spirals and hoops indicated that the spirals and hoops had yielded at the peak of the load-longitudinal strain curves or shortly after. This finding is independent of concrete compressive strength. Hence, it can be concluded that it is reasonable to take the nominal yield strength of the transverse steel when calculating the confining stress. Most of the strain gages on the high yield steel helices or spirals, however, indicated that the helices and spirals had not yielded at the peak of the load-longitudinal strain curves. This contradiction may be explained as follows: the effectively confined area of core concrete was significantly reduced due to incipient or serious buckling of longitudinal reinforcement at or near such a large longitudinal strain at peak stress where the ultra-high-strength transverse steel can yield. Also due to passive confinement, the damage of core concrete may have already been significant when the lateral pressure reached the maximum due to yielding of transverse reinforcement. On the other hand, in the case of Grade 430 reinforcement, the reinforcement can yield at a significantly smaller longitudinal strain of concrete and hence the effectively confined area will be at least as large as that estimated by the Mander, Priestley, and Park's method.[9] Also, additional confinement due to longitudinal reinforcement may also be expected unless the axial strain of longitudinal reinforcement greatly exceeds the yield strain. Therefore, the full yield strength of ultra-high steel cannot be used when calculating the confining stress.

Effect of confinement reinforcement configuration

The hoop configuration and the resulting distribution of the longitudinal steel play an important role in the confinement of concrete. In this study, it was possible to observe the effect of varying the hoop configuration. Comparing the behavior of Specimen 4A, constructed using single hoops, and Specimen 11A, confined using double hoop configuration, it was observed that Specimen 4A behaved in less ductile fashion with a sharp dropping of load. A similar comparison was made between Specimen 4B and 11B. In this case, the effect was even more pronounced, with Specimen 4B showing a pronounced reduction in load capacity after maximum load had been reached. These comparisons show that there was an improvement in the strength and ductility of the specimens as a result of better hoop configurations, indicating that the hoop configuration and the resulting distribution of the longitudinal steel play an important role in the confinement of concrete.

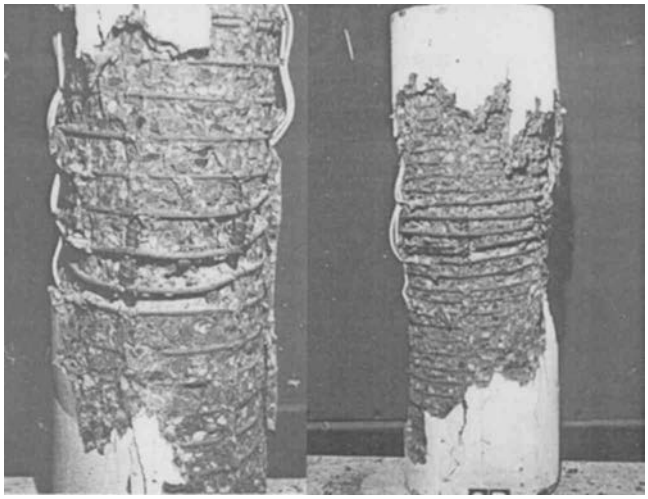

Fig. 10—Specimens with normal yield strength confining reinforcement after testing.

Effect of confining reinforcement spacing

To prevent early loss of strength of high-strength concrete columns, caused by both buckling of reinforcing bars and excessively deep arching of the confined concrete between the spirals or hoops, all columns should have sufficiently close spacing of transverse reinforcement. In this study, spacing of hoop or spirals varied from $1.66d_b$ to $5.83d_b$. Comparing the behavior of Specimen 2B ($s = 1.66d_b$) and Specimen 11A ($s = 5.14d_b$), the stress-strain curves of 2A and 11A (Fig. 4) show that as the hoop spacing was increased, the behavior became less ductile, the enhanced strength became smaller, and the longitudinal strain at the first hoop fractured decreased. Based on the test results of this study, the maximum pitch should not exceed $4d_b$ for normal yield strength steel if satisfactory behavior is to be achieved. A pitch of $6d_b$, however, will result in reasonable ductility. The same trend was observed for the high-strength concrete column confined by ultra high yield strength steel. It is recommended, therefore, that the maximum pitch should not be more than approximately $5d_b$ if satisfactory behavior is to be achieved.

Effect of volumetric ratio of confining reinforcement

From Fig. 4 to 7, the effect of the volumetric ratio of confining reinforcement on the behavior of the specimen is demonstrated. As expected, the larger the volumetric ratio of confining reinforcement, the more ductile the behavior of the specimen. For the confined specimen using high yield strength of transverse steel, the strength and ductility of the concrete were remarkably enhanced. This can been seen by comparing the test results of three specimens (1HA, 3HB1, and 3HC1) with the same volumetric ratio of confining reinforcement but with different concrete compressive strengths; the peak stress enhancements due to confinement were 2.04, 1.57, and 1.28, respectively. When the volumetric ratio was reduced to 1% level, the behavior of a high-strength concrete specimen was similar to that of an unconfined specimen. The test results indicted that a limitation on the minimum volumetric ratio of confining reinforcement is necessary to ensure ductile behav-

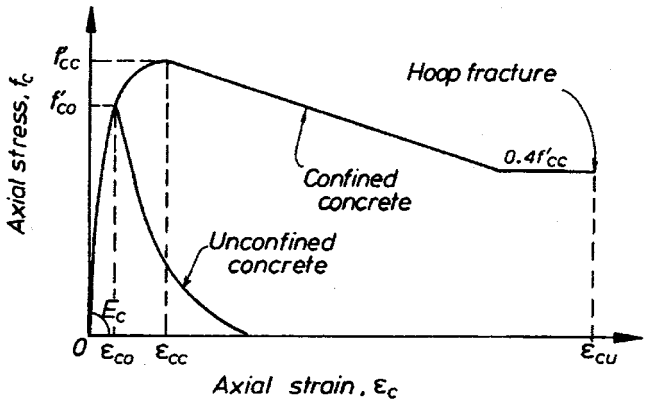

Fig. 11—Stress-strain relationship proposed for confined high-strength concrete.

ior of confined high-strength concrete, as was evident by the behavior of Specimens 10A, 10B, and so on.

Effect of amount of longitudinal steel

The confinement effectiveness is more dependent on the spacing of confining reinforcement than on the amount of longitudinal reinforcement. Thus, while doubling of the amount of longitudinal reinforcement improves the descending part of the curve, the improvement is not as significant as that obtained by decreasing the hoop spacing and volumetric ratio of confining reinforcement or changing the hoop configuration. Thus, it is apparent that the distribution of the longitudinal reinforcement in the column is more important for confinement effectiveness for a given amount of reinforcement. Also, there seems to be a limit on the amount of longitudinal reinforcement necessary for ductile behavior of confined high-strength concrete. There must not be less than eight longitudinal bars distributed along the perimeter of the column.

MODELING OF STRESS-STRAIN RELATIONSHIP OF CONFINED CONCRETE

The modeling of material stress-strain relationships is a basic requirement for the prediction of the behavior of structural elements. Theoretical moment-curvature analysis for reinforced concrete structural elements, indicating the available flexural strength and ductility can be constructed providing the stress-strain relations for the concrete and steel is known. The formulation of mathematical stress-strain relationships involves a large number of factors, particularly for high-strength concrete.

The principal factors considered in modeling the stress-strain relationships are as follows:

1. Type and strength of concrete;
2. Amount, pitch, and configuration of transverse reinforcement;
3. Amount and distribution of longitudinal reinforcement;
4. Mechanical properties of transverse and longitudinal reinforcement;
5. Ratio of confined area to gross area;
6. Monotonic and cyclic loading; and
7. Size and shape of confined concrete.

Monotonic loading curve

In the case of monotonic loading, it was not easy to find or derive a single polynomial function that fits well with all types of the stress-strain curves observed in tests described herein. The reason can be explained as follows: the confining effects are negligible in the initial part of the ascending branch of the stress-strain curve due to passive confinement of transverse reinforcement and small transverse strain. This means that the model curve needs to be changed little in the initial part of ascending branch but significantly altered near and after peak stress regions depending on the magnitude of confinement. It is hard to find a single polynomial function to satisfy such a condition.

In the case of a model that consists of several branches defined by different functions, it is easier to adjust the model curve to the experimental curve because the characteristics of ascending and descending branches can be controlled independently. Hence, the authors decided to establish a model by modifying the model proposed by Muguruma and Watanabe,[6] as shown as follows. The model consists of three branches expressed by Eq. (7) to (9) and a tail with a constant stress of $0.4f'_{cc}$.

When $0 \le \varepsilon_c \le \varepsilon_{co}$

$$f_c = E_c\varepsilon_c + \frac{(f'_{co} - E_c\varepsilon_{co})}{\varepsilon_{co}^2}\varepsilon_c^2 \tag{7}$$

when $\varepsilon_{co} \le \varepsilon_c \le \varepsilon_{cc}$

$$f_c = f'_{cc} - \frac{(f'_{cc} - f'_{co})}{(\varepsilon_{cc} - \varepsilon c_{co})^2} \times (\varepsilon_c - \varepsilon_{cc})^2 \tag{8}$$

when $\varepsilon > \varepsilon_{cc}$

$$f_c = f_{cc} - \beta\frac{f'_{cc}}{\varepsilon_{cc}} \times (\varepsilon_c - \varepsilon_{cc}) \ge 0.4f'_{cc} \tag{9}$$

A typical stress-strain curve of confined concrete determined by the model is schematically shown in Fig. 11. To draw the stress-strain curve of confined concrete using the previous equations, the maximum strength of confined concrete f'_{cc}, the axial strain at maximum strength ε_{cc}, and the β value, which controls the slope of the descending branch, need to be determined. The stress-strain curve is terminated at the ultimate compressive strain ε_{cu} where the first hoop fractures due to serious buckling of longitudinal bars. These variables are determined as follows.

Maximum strength of confined concrete f'_{cc}—In the last several decades, failure criteria associated with a maximum stress surface have been established for concrete under triaxial states of stress. Several numerical models, based on test results, have been proposed to represent this failure surface. In this study, the method used by Mander, Priestley, and Park[9] was employed. The five-parameters multiaxial failure criteria of William and Warnke[10] were used to describe the theoretical ultimate strength surface in this study. The tensile and compressive meridians are expressed as follows

$$\frac{\tau_{oct}}{f'_{co}} = a_0 + a_1\frac{\sigma_{oct}}{f'_{co}} + a_2\left(\frac{\sigma_{oct}}{f'_{co}}\right)^2 \tag{10}$$

at $\theta = 0$ degrees (tensile meridian)

$$\frac{\tau_{oct}}{f'_{co}} = b_0 + b_1\frac{\sigma_{oct}}{f'_{co}} + b_2\left(\frac{\sigma_{oct}}{f'_{co}}\right)^2 \quad (11)$$

at $\theta = 60$ degrees (compressive meridian)

Because attention is paid only to the compressive meridian, the equation of compressive meridian can be transformed as follows

$$\bar{\sigma}_{oct} = \frac{\sigma_1 + \sigma_2 + \sigma_3}{3f'_{co}} = -\frac{f'_{cc}}{3f'_{co}} - \frac{2f'_l}{3f'_{co}} \quad (12)$$

$$\bar{\tau}_{oct} = \frac{\sqrt{2}}{3f'_{co}}(f'_{cc} - f'_l) = -\sqrt{2}\left(\sigma_{oct} + \frac{f'_l}{f'_{co}}\right) \quad (13)$$

For triaxial case $\sigma_1 = \sigma_2 = f'_l$, then

$$\bar{\tau}_{oct} = b_0 + b_1(\bar{\sigma}_{oct}) + b_2(\bar{\sigma}_{oct})^2 \quad (14)$$

Substituting Eq. (12) into Eq. (14)

$$f'_{cc} = f'_{co}\left(\frac{3(b_1 + \sqrt{2}}{2b_2} + \right. \quad (15)$$

$$\left.\sqrt{\left(\frac{3(b_1 + \sqrt{2})}{2b_2}\right)^2 - \frac{9b_0}{b_2} - \frac{9\sqrt{2}}{b_2}\frac{f'_l}{f'_{co}}} + -2\frac{f'_l}{f'_{co}}\right)$$

Mander, Priestley, and Park[9] determined f'_{cc} using the test results of Schickert and Winkle[11] ($b_0 = 0.12229$, $b_1 = -1.15$, and $b_2 = -0.315$)

$$f'_{cc} = f'_{co}\left[-1.254 + 2.254\sqrt{1 + 7.94\frac{f'_l}{f'_{co}}} - 2\frac{f'_l}{f'_{co}}\right] \quad (16)$$

In this study, using the test results of Khaloo and Ahmad[12] for high-strength concrete, $b_0 = 0.113$, $b_1 = -1.26$, and $b_3 = -0.559$, and f'_{cc} for high-strength concrete was proposed as follows

$$f'_{cc} = f'_{co}\left[-0.413 + 1.413\sqrt{1 + 11.4\frac{f'_l}{f'_{co}}} - 2\frac{f'_l}{f'_{co}}\right] \quad (17)$$

In this study, f'_{cc} was established using the results of active confinement. The peak stresses of concrete under passive confinement with different stiffness, however, were always around the failure envelope of active confinement and the differences were found to be insignificant.[13] Therefore, it seems reasonable to consider that the difference between the active and passive confinement fracture envelope is negligible. In effect, the failure envelope could be considered to be stress path independent. Comparison between the previous equations is shown in Fig. 12. It is evident that the octahedral shear stress of high-strength concrete is smaller than that of normal-strength concrete at a given octahedral normal stress.

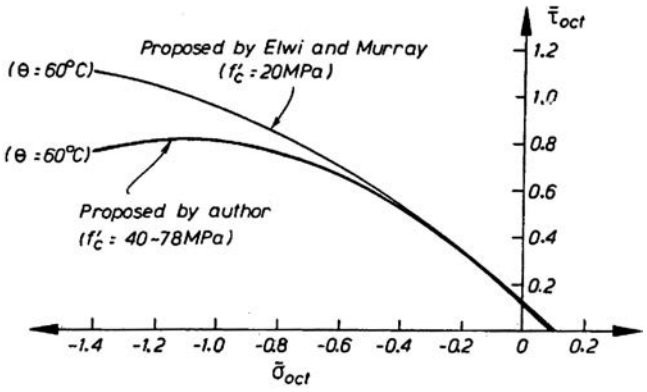

Fig. 12—Ultimate strength surfaces on octahedral plane.

For the properties of concrete confined by high yield strength steel, it should be noted that f'_l defined by Mander, Priestley, and Park[9] was based on the yield strength of the confining strength of the confining steel. The comparison between Mander, Priestley, and Park's model and the test results, however, show that the former model generally overestimated f'_{cc} for concrete confined by high yield strength steel. This is because the ultra high yield strength of steel is not developed until at high transverse strains, hence there is a delayed confining effect on the concrete relative to that provided by normal yield strength steel.

In this study, a regression analysis was conducted using the test results to modify the f'_l/f'_{co} value used to calculate f'_{cc}. Because the test results cover both confined normal- and high-strength concrete, Eq. (18) proposed by Mander, Priestley, and Park[9] was adopted for modification. The modification factor was found to be

$$f'_{cc} = f'_{co}\left[-1.254 + 2.254\sqrt{1 + 7.94\alpha_s\frac{f'_l}{f'_{co}}} - 2\alpha_s\frac{f'_l}{f'_{co}}\right] \quad (18)$$

$$\text{When } f'_{co} \le 52 \text{ MPa } \alpha_s = (21.2 - 0.35f'_{co})\frac{f'_l}{f'_{co}} \quad (19)$$

$$\text{When } f'_{co} > 52 \text{ MPa } \alpha_s = 3.1\frac{f'_l}{f'_{co}} \quad (20)$$

where f'_l is the effective lateral confining pressure, calculated using the equations proposed by Mander, Priestley, and Park, given as follows:

For circular confined section

$$f'_l = 0.5K_e\rho_s f_{yh} \quad (21)$$

For circular hoops

$$K_e = \frac{(1 - 0.5s'/d_s)^2}{1 - \rho_{cc}} \quad (22)$$

For spirals

$$K_e = \frac{(1 - 0.5s'/d_s)}{1 - \rho_{cc}} \quad (23)$$

For rectangular confined section:

The effective lateral pressure is given with good accuracy by

$$f_l' = 0.5K_e(\rho_x + \rho_y)f_{yh} \quad (24)$$

where

$$K_e = \frac{\left[1 - \sum_{i=1}^{n} \frac{C_i^2}{6b_c d_c}\right] \times \left[1 - 0.5\frac{s'}{b_c}\right] \times \left[1 - 0.5\frac{s'}{d_c}\right]}{1 - \rho_{cc}} \quad (25)$$

Axial strain at maximum strength e_{cc}—For circular confinement with ordinary-strength steel

$$\frac{\varepsilon_{cc}}{\varepsilon_{co}} = 1.0 + 384\left[\frac{f_l'}{f_{co}'}\right]^2 \quad (26)$$

For rectilinear confinement with ordinary-strength steel

$$\frac{\varepsilon_{cc}}{\varepsilon_{co}} = 1.0 + 11.3\left[\frac{f_l'}{f_{co}'}\right]^{0.7} \quad (27)$$

For circular confinement with ultra-high-strength steel

$$\frac{\varepsilon_{cc}}{\varepsilon_{co}} = 1.0 + (120 - 1.554f_{co}')\left(\frac{f_l'}{f_{co}'}\right) \text{ when } f_{co} \le 50 \text{ MPa} \quad (28)$$

$$\frac{\varepsilon_{cc}}{\varepsilon_{co}} = 1.0 + (71.4 - 0.623f_{co}')\left(\frac{f_l'}{f_{co}'}\right) \text{ when } f_{co}' > 50 \text{ MPa} \quad (29)$$

For rectilinear confinement with ultra-high-strength steel

$$\frac{\varepsilon_{cu}}{\varepsilon_{co}} = 2.0 + (87 - 1.06f_{co}')\sqrt{\frac{f_l'}{f_{co}'}} \text{ when } f_{co} \le 50 \text{ MPa} \quad (30)$$

$$\frac{\varepsilon_{cu}}{\varepsilon_{co}} = 2.0 + (53.4 - 0.42f_{co}')\sqrt{\frac{f_l'}{f_{co}'}} \text{ when } f_{co}' > 50 \text{ MPa} \quad (31)$$

Factor to control the slope of the descending branch b—For concrete confined by circular confinement

$$\beta = 0.2 \text{ when } f_{yh} \le 550 \text{ MPa and } f_{co}' \le 80 \text{ MPa} \quad (32)$$

$$\beta = 0.08 \text{ when } f_{yh} > 1200 \text{ MPa and } f_{co}' \le 80 \text{ MPa} \quad (33)$$

$$\beta = 0.2 \text{ when } f_{yh} > 1200 \text{ MPa and } f_{co}' > 80 \text{ MPa} \quad (34)$$

For concrete confined by rectilinear confinement

$$\beta = (0.048f_{co}' - 2.14) - (0.098f_{co}' - 4.57)\left(\frac{f_l'}{f_{co}'}\right)^{1/3} \quad (35)$$

$$\text{When } f_{yh} \le 550 \text{ MPa and } f_{co}' > 75 \text{ MPa} \quad (36)$$

$$\beta = 0.07 \text{ when } f_{yh} > 1200 \text{ MPa and } f_{co}' \le 80 \text{ MPa} \quad (37)$$

$$\beta = 0.1 \text{ when } f_{yh} > 1200 \text{ MPa and } f_{co}' > 80 \text{ MPa} \quad (38)$$

For rectilinear confinement with ordinary yield strength ($f_{yh} \le 550$ MPa), it was not possible to determine a uniform coefficient to fit all experimental curves. Therefore, the β value for each experimental curve was found using a trial-and-error method. The β values previously recommended do not cover all ranges of material strength with continuity, and hence, improvement in future research is expected.

Maximum concrete strain e_{cu}—The maximum concrete strain ε_{cu} has often been used in ductility calculations. Scott, Park, and Priestley[14] observed that it is reasonably conservative to define the limit of useful concrete compressive strain as the strain at which fracture of a hoop first occurs. In this study, the following empirical equations were proposed to estimate the ultimate compressive strain ε_{cu}, where the first hoop fractures occurs due to serious buckling of longitudinal bars.

For circular confinement with normal-strength steel

$$\frac{\varepsilon_{cu}}{\varepsilon_{co}} = 2 + (143.5 - 1.48f_{co}')\sqrt{\frac{f_l'}{f_{co}'}} \text{ when } f_{co}' < 80 \text{ MPa} \quad (39)$$

$$\frac{\varepsilon_{cu}}{\varepsilon_{co}} = 2 + (89.8 - 0.74f_{co}')\sqrt{\frac{f_l'}{f_{co}'}} \text{ when } f_{co}' \ge 80 \text{ MPa} \quad (40)$$

For rectilinear confinement with normal-strength steel

$$\frac{\varepsilon_{cu}}{\varepsilon_{co}} = 2 + (122.5 - 0.92f_{co}')\sqrt{\frac{f_l'}{f_{co}'}} \text{ when } f_{co}' < 80 \text{ MPa} \quad (41)$$

$$\frac{\varepsilon_{cu}}{\varepsilon_{co}} = 2 + (82.75 - 0.37f_{co}')\sqrt{\frac{f_l'}{f_{co}'}} \text{ when } f_{co}' \ge 80 \text{ MPa} \quad (42)$$

For circular confinement with ultra-high-strength steel

$$\frac{\varepsilon_{cu}}{\varepsilon_{co}} = 2.0 + (86.7 - 1.06f_{co}')\sqrt{\frac{f_l'}{f_{co}'}} \text{ when } f_{co}' \le 50 \text{ MPa} \quad (43)$$

$$\frac{\varepsilon_{cu}}{\varepsilon_{co}} = 2.0 + (53.5 - 0.42f_{co}')\sqrt{\frac{f_l'}{f_{co}'}} \text{ when } f_{co}' > 50 \text{ MPa} \quad (44)$$

For rectilinear confinement with ultra-high-strength steel

$$\frac{\varepsilon_{cu}}{\varepsilon_{co}} = 2.0 + (70.0 - 0.6f_{co}')\sqrt{\frac{f_l'}{f_{co}'}} \text{ when } f_{co} \le 50 \text{ MPa} \quad (45)$$

$$\frac{\varepsilon_{cu}}{\varepsilon_{co}} = 2.0 + (49.0 - 0.2f_{co}')\sqrt{\frac{f_l'}{f_{co}'}} \text{ when } f_{co}' > 50 \text{ MPa} \quad (46)$$

Figure 4 to 7 show comparisons between the experimental curves and theoretical curves determined using the previously described method. Overall the stress-strain model of con-

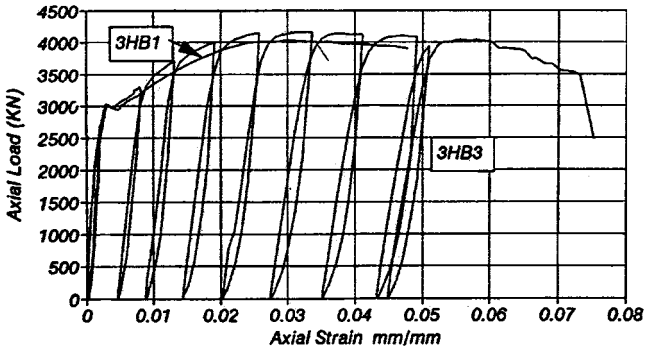

Fig. 13—Stress-strain curves of specimens under cyclic and monotonic loading conditions.

fined high-strength concrete proposed herein is quite close to the tested data, especially in the descending branch of the stress-strain curve.

It was also evident that none of the available high-strength concrete models are able to predict satisfactorily the measured stress-strain behavior of high-strength concrete confined by circular or rectangular transverse reinforcement with different yield strength. All the models predict the ascending branch of the stress-strain relationship fairly well, whereas the predicted descending branch of the curve is not consistent. All the models underestimated the maximum concrete strength, thus giving a very conservative stress-strain prediction for concrete confined by ultra high yield strength steel. More attention must be given to the following aspects, especially for the case of high-strength concrete.

1. It is notable that the magnitude of the compressive concrete strain measured in the postpeak stress region depends significantly on the gage length and location of strain measurement. This aspect does not relate directly to the confining effect but influences their assessment. Because the gage length and the location of strain measurement are different among researchers, it is difficult to compare data from different sources;

2. In the past tests on confined high-strength concrete, small scale models with less than 150 mm square section were used due to the limit of loading capacity of the testing machine. The difference in specimen size may also lead to difficulty in comparing test results from different sources; and

3. The relative stiffness of the testing machine and the concrete specimen is one of the key points, particularly for high-strength concrete. A flexible testing machine used close to its upper capacity will tend to snap back once peak load is reached, giving nonrepresentative results. This factor will make comparing the test results from different sources difficult.

Cyclic loading curves

For ordinary strength concrete confined by ordinary strength steel, it is normally assumed that the monotonic loading curve corresponds to the envelope curve of the stress-strain curves under cyclic loading. In this study, it was found that the assumption that the monotonic loading curve represents the skeleton curve of the stress-strain curves under cyclic loading is still valid, regardless of the concrete compressive strength and the yield strength of transverse reinforcement. Figure 13 shows the results for two specimens with the same confinement and nearly the same compressive strength of concrete tested under cyclic

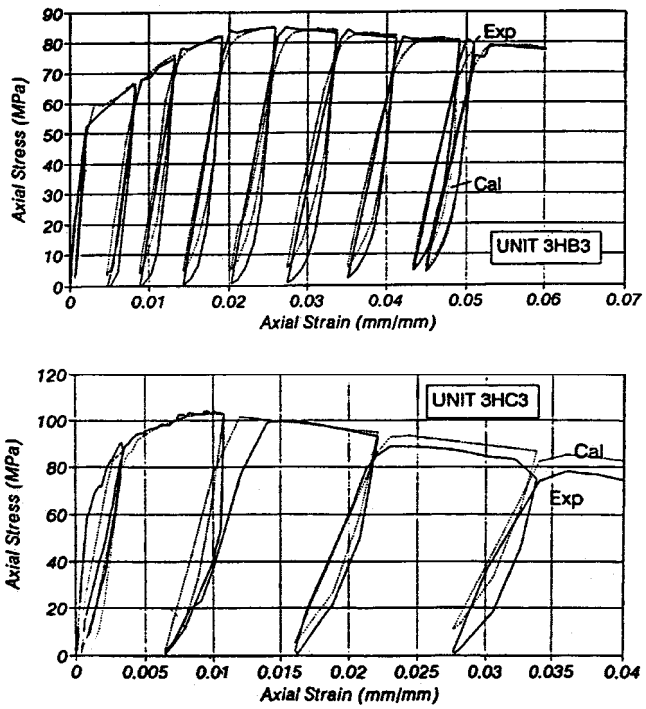

Fig. 14—Comparison of experimental and analytical cyclic stress-strain curves.

and monotonic loading conditions. Comparison between the experimental results and those predicted using the cyclic stress-strain model proposed by Mander, Priestley, and Park's[9] model modified by Dodd and Cooke[15] showed very good agreement (Fig. 14).

CONCLUSIONS

Based on the results of this investigation, the following conclusions can be drawn.

1. The most significant parameters affecting the shape of the stress-strain curve of confined high-strength concrete for all section shapes are the volumetric ratio and the yield strength of the confining reinforcement. As the yield strength of the confining reinforcement increases, the strength of the confined concrete also increases. The ultimate longitudinal strain was defined as the strain at first hoop or spiral fractured;

2. The influence of concrete compressive strength on the degree of column ductility is significant, particularly for concrete compressive strengths exceeding 60 MPa. Regardless of the concrete compressive strength, however, an increase in the confinement ratio increases the peak stress attained, increases the ultimate strain at first hoop or spiral fracture, and decreases the slope of the descending branching branch. An increase in the spacing of transverse reinforcement tends to reduce the efficiency of the confinement;

3. A stress-strain model for high-strength concrete confined using different types of normal-strength and high-strength confining reinforcement is proposed. The model is found to give reasonably good predictions of experimental behavior of circular and square specimens with high-strength concrete confined by either normal or high yield strength confining reinforcement with various configurations;

4. In axial loading tests on normal- and high-strength concrete cylinders and prisms confined by spirals or helices with

two ultra high and normal strength transverse reinforcement, the strength and ductility of the confined concrete was significantly enhanced when the ultra-high yield strength of steel was used. The expected general improvement of the behavior of confined high-strength concrete with confining reinforcement was observed in the tests;

5. To prevent a relatively early loss of strength of high-strength concrete caused by both buckling of reinforcing bars and excessively deep arching of the confined concrete in between the spirals and hoops, all specimens should have sufficiently close spacing of transverse reinforcement. A maximum pitch of $4d_b$ for Grade 430 transverse reinforcement or $5d_b$ for ultra-high-strength steel is recommended. For rectilinear confinement in high-strength concrete, the number of longitudinal bars must not be less than eight and those bars should be distributed along the perimeter of the column;

6. The analytical stress-strain model proposed in this paper was found to give reasonably good predictions of the experimental behavior of circular and square specimens with high-strength concrete confined by either normal or high yield strength confining reinforcement with various configurations; and

7. When cyclic and monotonic loading were applied to prisms and cylinders confined by transverse reinforcement with yield strength less than 500 MPa, the envelope skeleton of stress-strain curves coincided closely with the stress-strain curve obtained from a monotonic loading test, even for high-strength concrete specimens.

ACKNOWLEDGMENTS

Financial support from the Cement and Concrete Association of New Zealand, the New Zealand Concrete Society, Firth Certified Concrete, Pacific Steel Ltd., Koshuha-Netsuran Co. of Japan, Taisei Corp. of Japan, WG Grade (NZ) Ltd., and the New Zealand Ministry of External Relations and Trade is gratefully acknowledged.

NOTATION

d_b = nominal diameter of longitudinal reinforcing bar
d_c = diameter of confined concrete core of circular column section, measured to center-line of spiral or circular hoop
d_s = effective core diameter between circular hoop or spiral bar centers
E_c = Young's modulus of elasticity for concrete
E_s = Young's modulus of elasticity for steel
f_c = concrete stress
f_c' = specified concrete compressive strength
f_{cc}' = confined concrete compressive strength
f_{co}' = in-place unconfined concrete compressive strength
f_l = transverse confining stress
f_l' = effective transverse confining stress
f_y = yield strength of steel in tension
f_{yh} = yield strength of transverse reinforcing steel
K_e = confinement effectiveness coefficient, based on area ratio
s' = clear spacing between circular hoops or spirals
s_h = center-to-center spacing of spiral or hoop sets
ε_c = concrete compressive strain
ε_{cc} = strain at maximum confined strength of concrete f_{cc}'
ε_{co} = compressive strain at maximum in-place unconfined concrete strength f_{co}'
ε_{cu} = ultimate concrete compressive strain
ε_y = yield strain of steel
ρ_{cc} = volumetric ratio of longitudinal reinforcement in confined core concrete
ρ_s = volumetric ratio of confining reinforcement to core concrete
ρ_x = lateral confining steel parallel to *x*-axis
ρ_y = lateral confining steel parallel to *y*-axis

REFERENCES

1. Bing, L.; Park, R.; and Tanaka, H., "Strength and Ductility of Reinforced Concrete Members and Frames Constructed using High-Strength Concrete," *Research Report* 94-5, University of Canterbury, New Zealand, May 1994, 389 pp.

2. Martinez, S.; Nilson, A. H.; and Slate, F. O., "Spirally Reinforced High-Strength Concrete Columns," ACI JOURNAL, *Proceedings* V. 81, No. 5, Sept.-Oct. 1984, pp. 431-442.

3. Fafitis, A., and Shah, S. P., "Lateral Reinforcement for High-Strength Concrete Columns," SP-87, American Concrete Institute, Farmington Hills, Mich., 1985, pp. 213-232.

4. Yong, Y. Y.; Nour, M.; and Nawy, E. G., "Behavior of Lateral Confined High-Strength Concrete under Axial Loads," *Journal of Structural Engineering*, ASCE, V. 114, No. 2, 1988, pp. 332-350.

5. Bjerkeli, L.; Tomaszewicz, A.; and Jansen, J. J., "Deformation Properties and Ductility of High-Strength Concrete," *Proceeding of the Second International Symposium on Utilization of High-Strength Concrete*, University of California, Berkeley, Calif., May 1990.

6. Muguruma, H., and Watanabe, F., "Ductility Improvement of High-Strength Concrete Column With Lateral Confinement," *Proceedings of the Second International Symposium on Utilization of High-Strength Concrete*, Berkeley, Calif., 1990.

7. Cusson, D., and Paultre, P., "Stress-Strain Models for Confined High-Strength Concrete," ASCE, *Journal of Structural Engineering*, V. 121, No. 3, Mar. 1995.

8. Razvi, S., and Saatcioglu, M., "Confinement Model for High-Strength Concrete," ASCE, *Journal of Structural Engineering*, V. 125, No. 3, Mar. 1999.

9. Mander, J. B.; Priestley, M. J. N.; and Park, R., "Seismic Design of Bridge Piers," *Research Report* 84-2, Department of Civil Engineering, University of Canterbury, New Zealand, 1984, 444 pp.

10. William, K. L., and Warnke, E. P., "Constitutive Model for the Triaxial Behavior of Concrete," International Association for Bridge and Structural Engineering, *Proceedings*, V. 19, 1975.

11. Schickert, G., and Winkle, H., "Results of Tests Concerning Strength and Strain of Concrete Subjected to Multiaxial Compressive Stresses," *Deutscher Ausschuss Fur Stahlbeton*, Heft, 277, Berlin, Germany, 1977.

12. Khaloo, A. R., and Ahmad, S. H., "Behavior of High-Strength Concrete under Torsional Triaxial Compression," *ACI Materials Journal*, V. 86, No. 6., Nov.-Dec. 1989, pp. 550-558.

13. Sun, X.; Tan, T. H.; and Irawan, P., "Effect of Stress-Path on the Failure of Concrete under Triaxial Stress," *Proceedings of the EASEC-7 Conference*, Koichi, Japan, 1999.

14. Scott, B. D.; Park, R.; and Priestley, M. J. N., "Stress-Strain Behavior of Concrete Confined by Overlapping Hoops at Low and High Strain Rates," ACI JOURNAL, *Proceedings* V. 79, No. 1, Jan.-Feb. 1982, pp. 13-27.

15. Dodd, L. L, and Cooke, N., "The Dynamic Behavior of Reinforced Concrete Bridge Pier Subjected to New Zealand Seismicity," *Research Report* 92-6, Department of Civil Engineering, University of Canterbury, New Zealand, 1992, 460 pp.